RSC Advances

ROYAL SOCIETY OF CHEMISTRY

www.rsc.org/advances

COMMUNICATION

The influence of nanoparticles on enzymatic bioelectrocatalysis

Dmitry Pankratov,[a,b] Richard Sundberg,[c] Dmitry B. Suyatin,[c,d] Javier Sotres,[a] Alejandro Barrantes,[a] Tautgirdas Ruzgas,[a] Ivan Maximov,[c] Lars Montelius,[c,d] and Sergey Shleev*[a,b,e]

In nearly all papers concerning enzyme-nanoparticle based bioelectronic devices, it is stated that the presence of nanoparticles on electrode surfaces *per se* enhances bioelectrocatalysis, although the reasons for that 10 enhancement are often unclear. Here, we report detailed experimental evidence that neither an overpotential of bioelectrocatalysis, nor direct electron transfer and bioelectrocatalytic reaction rates for an adsorbed enzyme depend on the size of nanoparticles within the range of 20–80 15 nm, *i.e.* for nanoparticles that are considerably larger than the enzyme molecules.

Bioelectronics is a rapidly progressing interdisciplinary research field[1] that aims to integrate biomaterials and electronic elements into functional devices which, among many other applications, 20 can be used in high-tech, environmental, pharmaceutical and biomedical industries for sensing and power-generation purposes. High-performance direct electron transfer (DET)-based bioelectrocatalytic reactions at low overpotentials are needed to design sensitive, selective, and efficient third-generation (DET-25 based) bioelectronic devices, *e.g.* biosensors[2,3] and biofuel cells,[4,5] since third-generation bioelectronics are simple, non-toxic, and potentially miniaturisable down to nm scale. Nanostructuring electrode surfaces for enzyme-based bioelectronics is important because, in most cases, "planar" 30 biodevices, *i.e.* designed without artificial nano-decoration of electrodes, show very little or no electron transfer (ET) between immobilised redox enzymes and unmodified surfaces. The commonly offered explanation for "enzyme nano-wiring" is an appropriate orientation of proteins on nanomaterials for ET 35 reactions. Facile and effective bioelectrocatalysis has been shown in many papers, where different mono- and multi-centre redox enzymes, such as horseradish peroxidase,[6] glucose oxidase,[7-10] superoxide dismutase,[11] and cellobiose dehydrogenase,[12] with blue multi-copper oxidases (MCOs),[13-18] respectively, are 40 immobilised on different nanomaterials, *e.g.* metal and carbon nanoparticles (NPs) and nanotubes, graphene, nanoporous materials, *etc.* As a major proof for the enhancement of bioelectrocatalytic reactions, large bioelectrocatalytic currents that originate from nanostructured electrodes modified with 45 oxidoreductases are usually presented. However, it should be emphasised that electrocatalysis is not actually related to the current increase, but should result in the decrease of an overpotential, which is quite rarely addressed in the case of

bioelectrocatalytic reactions. Moreover, even for a particular 50 enzyme, *e.g. Trametes hirsuta* laccase (*Th*Lc), and a particular material, *e.g.* gold (Au), contradictory situations for different nanostructures can be found in the literature: the use of gold NPs (AuNPs) and nanoporous Au was shown to facilitate the DET-based bioelectrocatalytic reduction of oxygen (O_2),[13,18] whereas 55 Au-modified nano-/microstructured silicon chips with the immobilised enzyme displayed very limited DET-based activity.[19] Furthermore, two opposite dependences of bioelectrocatalytic currents that originate from O_2 bioelectroreduction on MCO-modified electrodes on NP size 60 have recently been reported.[20,21] These contradictions indicate difficulties in setting up an experimental system by which the effect of the size of NPs on the thermodynamics and kinetics of redox reactions at enzyme-NP modified electrodes can be indisputably addressed.

65 In this study, we explored two-dimensional (2D) sub-monolayer AuNP-modified electrodes to address whether NPs with a uniform size, which are significantly larger than the enzyme molecule (at least for times larger in diameter), affect bioelectrocatalysis. To the best of our knowledge, this is the first 70 description of the experimental model system in which the dependence of bioelectrocatalysis on NP size is solely probed. We clearly show that the registered overpotentials for a bioelectrocatalytic reaction on bare Au electrodes and Au electrodes modified with AuNPs of different sizes are almost 75 identical and also very close to the redox equilibrium potential of a catalysed half-reaction. Moreover, we present experimental data showing that bare Au electrodes modified with AuNPs do not exhibit any bioelectrocatalytic current dependence due to the sizes of the employed NPs, which have diameters between 20 and 80 80 nm, when the real surface area (A_{real}, also called microscopic or electrochemically active, as illustrated in Fig. 1a; details are in Supporting Information (SI)) of electrodes is taken into account for the analysis of bioelectrocatalytic signals. We monitored the bioelectroreduction of O_2 catalysed by an MCO adsorbed on the 85 modified electrodes. For our investigations, we chose a well-studied enzyme, *Myrothecium verrucaria* bilirubin oxidase (*Mv*BOx), which is widely used nowadays to design potentially implantable third-generation oxygen biosensors[22] and DET-based cathodes of biofuel cells.[4,17,23,24] Only AuNPs within the range of 90 20–80 nm were used to mitigate (*i*) quantum effects (electron coupling) in NPs (that are anticipated to be seen when employing metal particles with diameters below 5 nm) and (*ii*) to keep the

dependence of van der Waals forces between metal and protein surfaces on NP radius negligible.

Firstly, bare and AuNPs-modified Au electrodes were fabricated (Fig. 1b; SI). Contrary to previous studies, in which AuNPs were adsorbed by drop-coating on electrode surfaces,[13,17,20,21] aerosol AuNPs were deposited with an average density of 80 particles μm_{geom}^{-2} (*i.e.* number of particles per geometric area, A_{geom}, also called 2D projected area, Fig. 1a) on 100 nm thick Au film (Fig. 1b).
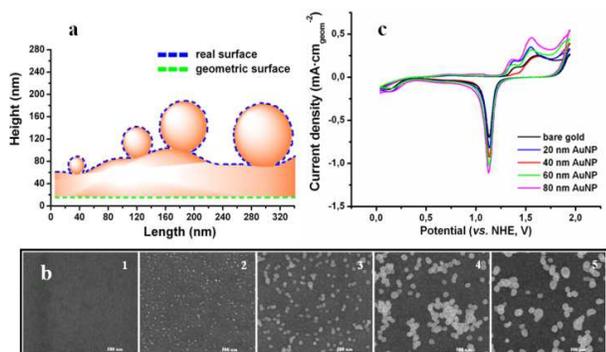

Figure 1. Characterisation of bare gold electrodes. (a) Comparison between real and geometric surface areas. (b) SEM images of bare electrode (1) and electrodes modified with 20 (2), 40 (3), 60 (4) and 80 (5) nm AuNPs. (c) Typical cyclic voltammograms of bare and AuNP-modified Au electrodes (0.5 M H_2SO_4, 100 mV s^{-1} scan rate, second cycle).

This procedure allowed the fabrication of nanostructured Au electrodes with AuNP sub-monolayers (Fig. 1b2-3) and avoided the formation of three-dimensional (3D) porous electrodes, which have additional uncontrolled nano-features. 3D electrodes based on AuNPs are unsuitable for the fundamental investigations aimed at in the present work since neither the shape nor size of nano-features inside porous structures are really known, whereas they are widely used to design selective BOx-based O_2 biosensors[22] and efficient biocathodes[4,17,24] nowadays. In the present work, the morphology, size, and AuNP density were carefully monitored before and after electrochemical measurements by using scanning electron microscopy (SEM). Due to the fabrication method, the AuNP-modified Au surfaces designed, although exhibiting some aggregation of NPs and a small variation in their sizes and shapes (Fig. 1b3-4), were very uniform compared to the nano-features of 3D porous electrodes fabricated by casting of chemically synthesised AuNPs to the electrode surface, followed by an electrochemical treatment (*cf.* Fig. 1b and, *e.g.*, Fig. 3 in ref.[23]). Moreover, contrary to previous studies, where only two (5 and 16 nm)[21] or three (7, 15, and 70 nm)[20] different NPs were used and two opposite dependences of bioelectrocatalytic currents on NP size were reported, four different diameters of NP with a uniform size step of 20 nm were exploited in the present work, *i.e.* Au electrodes were modified with 20, 40, 60, and 80 nm NPs (denoted AuNPs$_{20}$, AuNPs$_{40}$, AuNPs$_{60}$, and AuNPs$_{80}$, respectively; Fig. 1b). A_{real} of both bare and AuNPs-modified electrodes was estimated by using cyclic voltammetry measurements, *i.e.* commonly used procedure in Au electrochemistry (Fig. 1c; SI), which, along with A_{real} estimation, also allows Au surfaces to be clean and uniform on a molecular level.[25,26] Au electrodes were cycled in H_2SO_4 only twice to avoid

AuNP aggregation, deformation, and even disappearance (Supporting Fig. S1; additional details in ref.[23]). The experimentally obtained microscopic roughness factors (*f*) for bare Au electrodes, as well as electrodes modified with AuNPs$_{20}$, AuNPs$_{40}$, AuNPs$_{60}$, AuNPs$_{80}$, were found to be 1.8, 2.0, 2.1, 2.6, and 3.2, respectively (Fig. 1c; SI). These values are in agreement with theoretical *f* values (1.9, 2.2, 2.7, and 3.4 for AuNPs$_{20}$/Au, AuNPs$_{40}$/Au, AuNPs$_{60}$/Au, AuNPs$_{80}$/Au, respectively), which were calculated by taking into account A_{geom} of electrodes, AuNPs sizes and their average density on the electrode surfaces (Fig. 1a).

Secondly, *Mv*BOx was immobilised on bare polycrystalline "planar" (Fig. 1a; without modification with AuNPs) Au electrodes (*Mv*BOx/Au; SI). When electrochemical measurements of *Mv*BOx/Au were performed in O_2-containing buffer, an open-circuit potential (OCP) of O_2 bioelectroreduction was registered as 0.77 ± 0.02 V. Complete suppression of the bioelectrocatalytic current (Fig. 2a) in the presence of NaF, a well-known inhibitor of the O_2 (electro)reduction process catalysed by MCOs[27,28] (Fig. 2a), confirmed the bioelectrocatalytic origin of the obtained currents.
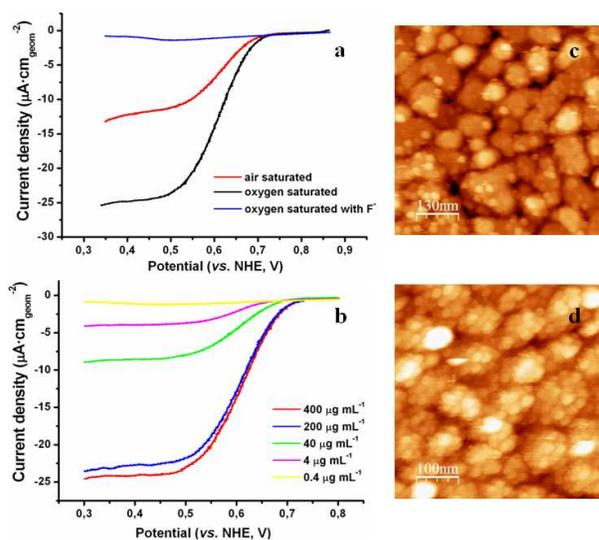

Figure 2. Characterisation of polycrystalline planar Au electrodes modified with *Mv*BOx. (a) Cyclic voltammograms (cathodic waves) of electrodes in air- and O_2-saturated PBS with and without 100 mM F$^-$ (20 mV s^{-1} scan rate, second cycle). (b) Voltammograms of electrodes modified with enzyme solutions of different concentrations (O_2-saturated PBS, 20 mV s^{-1} scan rate, second cycle). (c, d) AFM images of electrodes modified with dilute (c) and concentrated (d) solutions of the enzyme.

When the O_2 concentration was increased from 0.25 mM to 1.2 mM, by saturating of phosphate buffered saline (PBS) with O_2,[29] the maximal current density (j_{max}) of bioelectrocatalytic O_2 reduction increased by a factor of 2, *i.e.* from 12 μA cm$_{geom}^{-2}$ in air-saturated buffer to 25 μA cm$_{geom}^{-2}$ in O_2-saturated buffer (Fig. 2a). This result rules out serious O_2 diffusion limitations existing in the studies (details in SI), which could hinder possible dependences of the bioelectrocatalytic reaction on NP size. The dependence of biocatalytic currents on the *Mv*BOx surface concentration (Γ) was also studied. For this purpose, bare "planar" Au electrodes were modified with enzyme solutions of different concentrations. Bioelectrocatalytic signals significantly

increased up to 0.2 mg mL^{-1} of MvBOx used for biomodification (Fig. 2b), whereas a further increase in enzyme concentration had only a minor effect, which suggests full surface coverage, *i.e.* the formation of an enzyme monolayer on bare polycrystalline "planar" Au. To obtain additional information, atomic force microscopy (AFM) studies of Au electrodes modified with MvBOx using both dilute (0.25 mg mL^{-1}) and concentrated (4.0 mg mL^{-1}) enzyme solutions were performed (SI). When a concentrated enzyme solution was used for biomodification, full coverage of the electrode surface was obtained (Fig. 2d), supporting conclusions drawn from the electrochemical results, whereas a sub-monolayer coverage of the Au surface with protein molecules was registered when dilute MvBOx preparations were used (*cf.* Fig. 2c and 2d). In order to obtain quantitative data on MvBOx adsorption from the dilute preparation, ellipsometry studies were also carried out (SI). Γ value of about 3 pmol cm$_{real}^{-2}$ was calculated from experimental results (2.8 ± 0.1 mg m$_{geom}^{-2}$), taking into account the molecular weight of MvBOx and f of "planar" Au electrodes equal to 59 kDa and 1.8, respectively (SI). Finally, MvBOx was immobilised on AuNP-modified Au electrodes (MvBOx/AuNPs/Au). Pronounced bioelectrocatalytic reduction of O$_2$ on MvBOx/AuNPs/Au occurred when biomodified electrodes were placed in O$_2$-saturated buffer (Fig. 3a). OCPs of MvBOx/AuNPs/Au in O$_2$-containing buffers were also found to be 0.77±0.02 V, respectively, without any statistically relevant dependence of the registered values on AuNP size. Sub-monolayer coverage of AuNPs and MvBOx along with high O$_2$ concentration in solution was also used to eliminate possible mass transfer limitations. On the one hand, clear dependence of j_{max} values on AuNP sizes was registered (Fig. 3a). On the other hand, when CVs were plotted using A_{real}, very similar j_{max} values of about 15±3 µA cm$_{real}^{-2}$ were obtained (Fig. 3b). Since unmodified, identically cleaned, and also chemically uniform Au surfaces were used in our studies, it is also reasonable to assume an identical Γ value equal to 3 pmol cm$_{real}^{-2}$ for both bare Au and AuNP-modified Au electrodes. By taking into account this value, standard heterogeneous ET (k_0) and apparent bioelectrocatalytic constants (k_{cat}^{app}) (Fig. 3c) were calculated by using mathematical modelling studies (modeled curves are presented in Fig. 3a; details are in SI). The biocatalytic constant (k_{cat}) for MvBOx adsorbed on Au surface, *i.e.* the apparent bioelectrocatalytic constant (k_{cat}^{app}), was calculated to be *ca.* 14 s^{-1} (Supporting Table S1), whereas k_{cat} in homogeneous catalysis was measured to be 57 s^{-1} using 2,2'-azino-bis(3-ethylbenzthiazoline-6-sulphonic acid) (ABTS^{2-}) as an electron donor (reactions are illustrated in Fig. 3d; details in SI). Different but still comparable k_{cat} and k_{cat}^{app} values show that MvBOx is only partially deactivated/denatured on the bare metal surface. Importantly, both k_0 and k_{cat}^{app} values in the case of MvBOx/Au and MvBOx/AuNPs/Au electrodes are very close to each other, *viz.* 10.4±0.4 s^{-1} *vs.* 15.0±1.5 s^{-1}, respectively (Fig. 3c). It appears that biocatalytic activity of adsorbed MvBOx, *i.e.* k_{cat}^{app} values, does not depend on electrode modification with AuNPs in general, and NP diameters in particular. In all likelihood, the observed quite negligible difference in calculated k_{cat}^{app} values is related to experimental artefacts and equalised parameters used during mathematical modelling, *e.g.* assumption of an identical Γ value for all electrodes. Actually, since OCP values measured for

MvBOx/Au and MvBOx/AuNPs/Au electrodes were almost identical and independent of NP size, no decrease in overpotential, which was found to be only *ca.* 0.02 V, due to the presence of AuNPs on the electrode surface was registered, *i.e.* no real enhancement of electrocatalysis was observed in our studies. Moreover, even for MvBOx/Au, measured OCP values (0.77 ± 0.02 V) were very close to the redox equilibrium potential of O$_2$/H$_2$O couple (0.79 V at pH 7.4, 25°C) and could not be increased further significantly due to the pure thermodynamics. Importantly, Fig. 3c clearly demonstrates the independence of k_0 from AuNP diameters, *i.e.* DET rates do not depend on NP size for this system. Moreover, almost identical k_0 values were obtained for MvBOx/Au and MvBOx/AuNPs/Au (10.7±0.3 s^{-1} *vs.* 10.3±0.5 s^{-1}). Thus, all of the experimental data point to the fact that nanostructuring significantly improved bioelectrocatalytic signals only due to an increase in the value of A_{real} (*cf.* Fig. 3a and 3b), *i.e.* that NPs *per se* do not enhance enzymatic bioelectrocatalysis in general, and DET in particular.
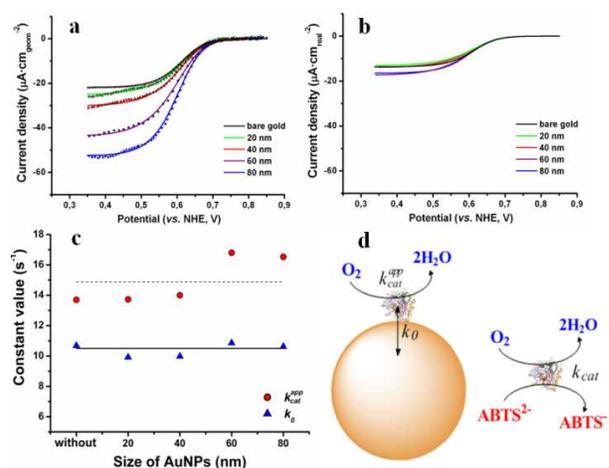

Figure 3. Characterisation of bare and AuNP-modified Au electrodes with immobilised MvBOx. (a, b) Experimental *vs.* modelled voltammograms of electrodes in O$_2$-saturated PBS (points – experimental data, lines – modelled curves; enzyme solution with concentration equal to 0.2 mg mL^{-1} was used for biomodification; 20 mV s^{-1} scan rate, second cycle). (c) Dependence of calculated biocatalytic constants (k_0 and k_{cat}^{app}) on AuNPs. (d) Schematic illustration of bio(electro)catalytic reduction of O$_2$ in heterogeneous and homogeneous systems.

We would like to emphasise that our results cannot be directly extrapolated to all cases, *e.g.* different NPs and other oxidoreductases, because only one particular redox enzyme and only bare metal NPs were used in the current work. Moreover, only Au nanostructures in the range of 20–80 nm, *i.e.* significantly larger than the enzyme molecule, were investigated herein. In our recent work, an enhancement of DET rates for ThLc-modified electrodes by the use of functionalised AuNPs, that are comparable with the size of the enzyme molecules, was demonstrated.[21] Thus, the improvement of bioelectronic devices on a nanoscale level is achieved *via* NPs comparable or less than enzyme molecules, as they enable to reduce an electron tunnelling distance of the electron transfer pathway, or/and *via* functionalised NPs, since they protect enzymes from deactivation on bare surfaces.[3,7,21,30] It should be emphasised that the improved bioelectrocatalysis might be achieved by employing NPs that are larger than enzyme molecules, *e.g.* by the use of chemically

synthesised NP preparations, which might contain a very minor fraction of small NPs that are comparable with the size of oxidoreductases. The formation of nanocavities in porous electrodes or because of NP-NP interactions on "planar" surfaces, when using large NPs, might also facilitate bioelectrocatalysis due to possible enzyme stabilisation.[31] To avoid all of these complications in our studies, nanostructured surfaces with sub-monolayers of NPs were used, *i.e.* possibilities for NP-NP interactions are significantly reduced and the formation of nanoporous structures was very unlikely. Thus, pure dependences of thermodynamic parameters and kinetic constants of the bioelectrocatalytic reaction on AuNP diameter could be clearly addressed.

Conclusions

Using model systems, *i.e.*, 2D electrodes based on NP sub-monolayers, we demonstrated without a doubt that the improved bioelectrocatalytic signals, when employing NPs larger than the enzyme molecule, are just a factor of the inherent area magnification by employing nanostructures. The size of the NPs in this size domain does not affect the bioelectrocatalytic properties of the NP-enzyme conjugate. In general, careful characterisation of DET based bioelectrocatalysis, when complex nanobioassemblies are investigated, is extraordinarily difficult, but important for scientific progress and the commercial feasibility of third-generation bioelectronics based on nano-wired oxidoreductases.

Acknowledgements

Notes and references

[a] Biomedical Sciences, Health & Society, Malmö University, 205 06 Malmö, Sweden; E-mail: sergey.shleev@mah.se
[b] Kurchatov NBICS Centre, National Research Centre "Kurchatov Institute", 123182 Moscow, Russia
[c] Division of Solid State Physics and The Nanometer Structure Consortium (nmC@LU), Lund University, 221 00 Lund, Sweden
[d] Neuronano Research Center, Lund University, 221 00 Lund, Sweden
[e] A .N. Bach Institute of Biochemistry, 119071 Moscow, Russia

† Electronic Supplementary Information (ESI) available: Additional information about chemicals and equipment, fabrication and characterization of electrodes, redox enzyme, biomodification; AFM and electrochemical investigations; theoretical basis of measurements and modeling studies. See DOI: 10.1039/b000000x/

1   I. Willner, E. Katz, Eds, *Bioelectronics: From Theory to Applications*, Wiley-VCH, Weinheim, Germany, 2005.

2   L. Murphy, *Curr. Opin. Chem. Biol.*, 2006, **10**, 177-184.

3   I. Willner, R. Baron and B. Willner, *Biosens. Bioelectron.*, 2007, **22**, 1841-1852.

4   M. Falk, Z. Blum and S. Shleev, *Electrochim. Acta*, 2012, **82**, 191-202.

5   Y. Liu, Y. Du and C. M. Li, *Electroanalysis*, 2013, **25**, 815-831.

6   J. Zhao, R. W. Henkens, J. Stonehuerner, J. P. O'Daly and A. L. Crumbliss, *J. Electroanal. Chem.*, 1992, **327**, 109-119.

7   Y. Xiao, F. Patolsky, E. Katz, J. F. Hainfeld and I. Willner, *Science*, 2003, **299**, 1877-1881.

8   A. Guiseppi-Elie, C. Lei and R. H. Baughman, *Nanotechnology*, 2002, **13**, 559-564.

9   B. Haghighi and M. A. Tabrizi, *Electrochim. Acta*, 2011, **56**, 10101-10106.

10   P. Wu, Q. Shao, Y. Hu, J. Jin, Y. Yin, H. Zhang and C. Cai, *Electrochim. Acta*, 2010, **55**, 8606-8614.

11   M. S. El-Deab and T. Ohsaka, *Electrochem. Commun.*, 2007, **9**, 651-656.

12   F. Tasca, L. Gorton, W. Harreither, D. Haltrich, R. Ludwig and G. Noll, *J. Phys. Chem. C*, 2008, **112**, 9956-9961.

13   M. Dagys, K. Haberska, S. Shleev, T. Arnebrant, J. Kulys and T. Ruzgas, *Electrochem. Commun.*, 2010, **12**, 933-935.

14   U. B. Jensen, M. Vagin, O. Koroleva, D. S. Sutherland, F. Besenbacher and E. E. Ferapontova, *J. Electroanal. Chem.*, 2012, **667**, 11-18.

15   M. C. Weigel, E. Tritscher and F. Lisdat, *Electrochem. Commun.*, 2007, **9**, 689-693.

16   W. Zheng, Q. Li, L. Su, Y. Yan, J. Zhang and L. Mao, *Electroanalysis*, 2006, **18**, 587-594.

17   K. Murata, K. Kajiya, N. Nakamura and H. Ohno, *Energy Environ. Sci.*, 2009, **2**, 1280-1285.

18   U. Salaj-Kosla, S. Poller, W. Schuhmann, S. Shleev and E. Magner, *Bioelectrochemistry*, 2013, **91**, 15-20.

19   A. Ressine, C. Vaz-Dominguez, V. M. Fernandez, A. L. De Lacey, T. Laurell, T. Ruzgas and S. Shleev, *Biosens. Bioelectron.*, 2010, **25**, 1001-1007.

20   M. Suzuki, K. Murata, N. Nakamura and H. Ohno, *Electrochemistry (Tokyo)*, 2012, **80**, 337-339.

21   C. Gutierrez-Sanchez, M. Pita, C. Vaz-Dominguez, S. Shleev and A. L. De Lacey, *J. Am. Chem. Soc.*, 2012, **134**, 17212-17220.

22   M. Pita, C. Gutierrez-Sanchez, M. D. Toscano, S. Shleev and A. L. De Lacey, *Bioelectrochemistry*, 2013, **94**, 69–74.

23   V. Andoralov, M. Falk, B. Suyatin Dmitry, M. Granmo, J. Sotres, R. Ludwig, O. Popov Vladimir, J. Schouenborg, Z. Blum and S. Shleev, *Sci. Rep.*, 2013, **3**, 3270.

24   X. Wang, M. Falk, R. Ortiz, H. Matsumura, J. Bobacka, R. Ludwig, M. Bergelin, L. Gorton and S. Shleev, *Biosens. Bioelectron.*, 2012, **31**, 219-225.

25   U. Oesch and J. Janata, *Electrochim. Acta*, 1983, **28**, 1237-1246.

26   S. Trasatti and O. A. Petrii, *Pure Appl. Chem.*, 1991, **63**, 711-734.

27   J. A. Cracknell, K. A. Vincent and F. A. Armstrong, *Chem. Rev.*, 2008, **108**, 2439-2461.

28   S. Shleev, J. Tkac, A. Christenson, T. Ruzgas, A. I. Yaropolov, J. W. Whittaker and L. Gorton, *Biosens. Bioelectron.*, 2005, **20**, 2517-2554.

29   G. A. Truesdale and A. L. Downing, *Nature*, 1954, **173**, 1236.

30   B. Willner, E. Katz and I. Willner, *Curr. Opin. Biotechnol.*, 2006, **17**, 589-596.

31   H.-X. Zhou and K. A. Dill, *Biochemistry*, 2001, **40**, 11289-11293.